Measurement report: The variation properties of aerosol hygroscopic growth related to chemical composition during new particle formation days in a coastal city of southeast China

Lingjun Li[1,2,3], Mengren Li[1,2,3*], Xiaolong Fan[1,2,3], Yuping Chen[1,2,3], Ziyi Lin[1,2,3], Anqi Hou[1,2], Siqing Zhang[1,2,3], Ronghua Zheng[1,2,3], Jinsheng Chen[1,2,3*]

[1] Institute of Urban Environment, Chinese Academy of Sciences, Xiamen 361021, China;

[2] Fujian Key Laboratory of Atmospheric Ozone Pollution Prevention, Institute of Urban Environment, Chinese Academy of Sciences, Xiamen 361021, China;

[3] College of Resources and Environment, University of Chinese Academy of Sciences, Beijing 100086, China

* Corresponding to: Jinsheng Chen (jschen@iue.ac.cn) and Mengren Li (mrli@iue.ac.cn)

Abstract. The scattering of solar radiation by aerosol is significantly affected by relative humidity (RH) due to the aerosol hygroscopicity. In order to better understand the characteristics of aerosol scattering hygroscopic growth and its influencing factors during new particle formation (NPF) days, we conducted the in-situ campaign from February to April 2022 in Xiamen, a coastal city in southeastern China. The aerosol scattering hygroscopic growth factor *f*(RH), commonly used to describe the aerosol indirectly hygroscopicity, varies greatly due to the influence of aerosol chemical composition and size. In the relatively clean atmosphere of Xiamen, NPF events occur frequently, and the variation in chemical composition during the events has a substantial influence on the aerosol scattering hygroscopic growth. In this study, we investigated the features and influencing factors of *f*(RH) in the NPF days. The research results emphasized that *f*(RH) differed significantly between NPF and non-NPF days, mainly impacted by the aerosol chemical compositions, especially sulfate and nitrate. In the NPF days, sulfate was the dominant contributor to *f*(RH), distinguishing from the non-NPF days. Aerosol hygroscopicity-chemical composition closure demonstrated that NH_4HSO_4 was the main driving force (30.78%) of the hygroscopicity parameter $\kappa_{f(RH)}$ when NPF events happened, while NH_4NO_3 played a dominant role in $\kappa_{f(RH)}$ (up to 35%) for non-NPF days. Although the uncertainty of the organic aerosol (OA) to hygroscopicity might exist due to the varieties of chemical components and oxidation level, it was the crucial driving factor for the variation in aerosol hygroscopicity. The findings of this study would be helpful for the further understanding about the properties of aerosol hygroscopicity in the coastal area, as well as complementing the hygroscopic growth factors to the models of air quality and climate change.

1 Introduction

Atmospheric aerosols have direct and indirect effects on atmospheric visibility, the earth-atmosphere radiation budget, clouds and precipitation, which in turn affect climate (Charlson et al., 1992); and these effects are strongly dependent on the hygroscopic properties of the ambient aerosol and the relative humidity (RH). The aerosol optical properties are key parameters for accurately estimating the direct radiative forcing caused by aerosols in climate models (IPCC, 2021). The aerosol hygroscopicity has a significant impact on the optical properties by altering particle size and refractive index, and ultimately on the climatic and environmental effects of aerosols (Covert et al., 1972; Tang, 1996; Malm and Day, 2001). Particles absorb water through hygroscopic growth, growing to sizes that are more efficient for light scattering, and their refractive index changes, resulting in enhanced aerosol scattering (Seinfeld et al., 1998). The aerosol liquid water content (ALWC) increases as particles absorb water in humid environment due to aerosol hygroscopicity. The condensed water in aerosols serves as an effective medium for multiphase chemistry, promoting the transformation of active gaseous pollutants into particles. Meanwhile, the newly formed hygroscopic aerosol components, such as secondary aerosols, can also alter aerosol hygroscopic

behaviors and enhance aerosol extinction efficiency. These processes lead to regional visibility impairment and accelerated formation of heavy haze. Therefore, aerosol hygroscopicity can profoundly affect atmospheric chemical processes (Wu et al., 2018) and air quality (Liu et al., 2020a).

Aerosol hygroscopic growth become the main factors affecting the aerosol optical properties at high ambient humidity due to the enhanced aerosol hygroscopicity and increased RH (Jin et al., 2022). The aerosol scattering hygroscopic growth factor (f(RH)) is defined as the ratio of aerosol scattering coefficient at an elevated RH level (σ_{sp}(RH, λ)) to that under dry condition (σ_{sp}(RH_{dry}, λ)) (usually RH < 40 %) at a given wavelength. The scattering enhancement owing to hygroscopic growth strongly depends on the source of the aerosol, which varies in chemical composition (Yan et al., 2009;Sheridan et al., 2002;Fierz-Schmidhauser et al., 2010a;Kotchenruther and Hobbs, 1998). For example, marine aerosols tends to have higher f(RH) than urban or continental aerosols, and their f(RH) decreases under strong anthropogenic influence (Zieger et al., 2010; Yan et al., 2009; Sheridan et al., 2001). Mineral dust and freshly emitted biomass combustion aerosols exhibit the lowest f(RH) values among the aerosol types studied (Sheridan et al., 2002;Pan et al., 2009;Fierz-Schmidhauser et al., 2010a). Hydrophilic species such as secondary inorganic components, sea salts, and water-soluble organics in the aerosol are the main contributors to the hygroscopic growth (Li et al., 2021; Fierz-Schmidhauser et al., 2010a), while black carbon and some organic carbons are the major proportion of the hydrophobic species (Liu and Zhang, 2010). Thus, discrepancies in the chemical composition of the aerosol, the fraction of soluble and insoluble chemical components, i.e., lead to variations of f(RH) (Malm et al., 2005;Zieger et al., 2014;Zhang et al., 2015). Additionally, particle number size distribution (PNSD) is another factor affecting f(RH). For a fixed chemical composition, f(RH) decreases with increasing particle size (Fierz-Schmidhauser et al., 2010b; Zieger et al., 2010; Baynard et al., 2006). Particle morphology, including shape and mixing state, significantly affects aerosol hygroscopicity. Giordano et al. (2015) demonstrated that the non-spherical shape of particles not only influences their hygroscopic behavior, but also changes in the mixing state of particles—whether they are internally or externally mixed—influence their hygroscopic properties (Stevens and Dastoor, 2019). Noted that the aerosol chemical compositions, particle sizes and morphology have a combined impact on f(RH) in the atmospheric environment, as the two are closely related (Wu et al., 2017; Kreidenweis and Asa-Awuku, 2014).

The observation site is situated in Xiamen, a fast-urbanization coastal city in southeastern China, at the junction of land and sea. As a result of massive population growth and rapid economic development, its atmospheric environment is subjected to complex pollution situations, such as the increased atmospheric oxidation (Liu et al., 2022) and relative high nitrogen oxide pollution (Chen et al., 2023). Notably, despite these conditions, aerosol concentrations remain generally lower compared to those in highly polluted megacities in China, according to open-access data from China Environmental Monitoring Centre (https://www.zq12369.com/index.php). On the other

hand, it is located at a subtropical city with a relative high air temperatures and high RH. High RH not only directly increases light scattering, leading to the decline of visibility (Won et al., 2021), but also affects the aerosol chemical processes involved in the particle formation(Sun et al., 2013; Chen et al., 2021). New particle formation (NPF) events occur frequently in this coastal city in southeast China with relative clean air quality (Wang et al., 2022). NPF is a process that low-volatile compounds emitted from natural or anthropogenic sources form into thermodynamically stable molecular clusters and grow into larger particles via condensation or collision with other vapours or particles (Holmes, 2007). When NPF occurs, both the PNSD and the chemical composition of the aerosol undergo significant changes, which have a remarkable influence on the aerosol hygroscopicity and *f*(RH). Previous studies of *f*(RH) had been conducted mainly in the megacity agglomerations such as North China Plain, Yangtze River Delta and Pearl River Delta (Liu et al., 2012; Xia et al., 2019; Ding et al., 2021; Jin et al., 2022; Zhao et al., 2019a), while limited attention had been paid to the southeast coastal areas with relative low level of particle and high RH. Meanwhile, these studies have focused more on the effect of aerosol chemical composition on *f*(RH) (Li et al., 2021; Wang et al., 2021; Jin et al., 2022), however, the exploration to the variation of *f*(RH) during NPF days is quite few in China.

In order to investigate the characteristics of *f*(RH) and its influencing factors during the NPF days, the enhanced observations utilized a high-resolution, humidified nephelometer system combined with the PNSD instruments to measure *f*(RH) for RH ranging from 40% to 91% in urban Xiamen. Routine measurements including other aerosol chemical and physical properties were also synchronously conducted. Differences and variations in *f*(RH) between NPF and non-NPF days were explored and the effect of aerosol chemical compositions on *f*(RH) were also discussed. The research was expected to characterize the properties of aerosol hygroscopicity during the NPF and non-NPF days in coastal area with relative low level of particle and high RH, and provide references to the model improvement for air quality and climate change.

2 Instruments and methods

2.1 Observation site

The enhanced observations were carried out at the Institute of Urban Environment of the Chinese Academy of Sciences in Xiamen (IUE, CAS), which is situated on the west coast of the Taiwan Strait. The observation station (118°03′E, 24°36′N) was located on the roof of an 80m-heigh building, a typical urban site surrounded by two main trunk roads (Jimei main road and Haixiang express road), shopping malls, educational institutions, and residential areas, and there was no apparent industrial emission sources nearby. Thus, the collected data can accurately represent the average air quality levels in the urban area of Xiamen. The observations were conducted consecutively from the 1st February to the 30th April 2022.

2.2 Observation instruments

The *f*(RH) values were obtained using a multi-band dual-nephelometer system

(PB-FRH100, BMET, China) comprising a nephelometer for aerosol scattering coefficients under dry conditions and another nephelometer for humidified aerosols. The airflow initially passed through two tandem Nafion dryers which could decrease the RH of the airflow to less than 30%. After this, the airflow was divided into two routes, one was directed straight into the nephelometer, while the other was humidified via a Gore-Tex tube set in a stainless steel tube before flowing into the nephelometer. The space between these two tubes contained circulating water, which was heated by two water baths. The scattering coefficients of dry and humidified $PM_{2.5}$ were measured at three wavelengths (450, 525 and 635 nm) using two nephelometers. The detailed principles and operation of the system has been described in Supplement material (Text S1). This study set the minimum and maximum RH at 40% and 91%, respectively, with a 45-minute cycle for humidification.

An integrating nephelometer (Aurora-3000, Ecotech, Australia) was used to simultaneously and continuously measure the 5-min average σ_{sp} at the same three wavelengths, and the σ_{sp} at 525 nm was appropriate for characterizing the aerosol scattering coefficient in this study. A Scanning Mobility Particle Sizer (SMPS, model 3938 L50, TSI Inc., USA), integrated with a Differential Mobility Analyzer (DMA, model 3082, TSI Inc., USA), a butanol-based Condensation Particle Counter (CPC, model 3750, TSI Inc., USA) and an aerosol neutralizer, were used to continuously measure the PNSD in the range of 7-300 nm over a 5-minute scanning interval during the measurement. The hourly chemical composition of aerosol, including sulfate (SO_4), nitrate (NO_3), ammonium (NH_4), chloride (Chl) and organics (Org), was measured by a high-resolution Aerodyne Aerosol Chemical Speciation Monitor (Q-ACSM). The relative ion efficiency (RIE) for SO_4, NO_3, NH_4, Chl and Org was 0.53, 1.1, 5.49, 1.3 and 1.4, respectively. PMF/ME-2 models were performed to identify OA factors resolving primary organic aerosol (POA) and secondary organic aerosol (SOA) in this study. POA is the unoxygenated component, and SOA is a more oxygenated organic aerosol. More detailed descriptions on the PMF analysis are given in Text S2. An AE-31 aethalometer (Magee Scientific, USA) was used to measure the balck carbon (BC) aerosol concentrations. Hourly mass concentrations of $PM_{2.5}$ and PM_1 were measured by a Tapered Element Oscillating Microbalance (TEOM1405, Thermo Scientific Corp., USA). Ambient meteorological parameters, including air temperature (T), RH, wind speed (WS) and wind direction (WD), were continuously monitored by an ultrasonic weather station instrument (150WX, Airmar, USA). Gaseous pollutants (carbon oxide, sulfur dioxide, and nitrogen dioxide) were measured by online Thermo Instruments TEI 48i, 49i, 43i, and 42i (Thermo Scientific Corp., USA).

2.3 Identification and classification of new particle formation

The NPF process involves nucleating and growing. The particles nucleated at a critical size of approximately 1.5 ± 0.4 nm (Kulmala et al., 2012) and then could grow into larger particles. During the sampling period, a total of 85 days of valid observations were available for PNSD analysis. The particles were divided into three modes:

nucleation mode (< 25 nm), Aitken mode (25-100 nm) and accumulation mode (> 100 nm) in this study (Kalkavouras et al., 2021; Shen et al., 2022; Wang et al., 2022). To identify NPF events, the visual analysis of PNSD data described by Dal Maso et al. (2005) was used. If a new particle mode is observed in the nucleation mode within a few hours and the mode shows clear signs of growth, characterized by a distinct "banana" shape in the time series of PNSD, then the day can be classified as an NPF event day. With the exception of NPF days, all other days are classified as non-NPF days or Undefinded days. Non-NPF days are confirmed when there is clearly no evidence of NPF or when the above criteria are not met. Besides, days that can not fulfil the criteria to be identified as NPF or non-NPF days were classified as Undefined days, and they are characterised by the presence of some particles in the nucleation mode with no visible signs of growth, or by the observation of growth not in the nucleation mode.

2.4 Data processing

The scattering Ångström exponent (α) indicates the wavelength dependence of aerosol scattering, and the parameters related to aerosol size are relatively low for large particles and relatively high for small particles(Guan et al., 2021). It is expressed as follows:

$$\alpha = \frac{\log(\sigma_{sp,\lambda_1}) - \log(\sigma_{sp,\lambda_2})}{\log(\lambda_1) - \log(\lambda_2)} \quad (1)$$

Where, λ_1=450 nm and λ_2=635 nm in this study.

The overall hygroscopicity parameter $\kappa_{f(RH)}$ can be obtained from the measured f(RH). The detailed calculation procedure of this method is shown in Supplement material (Text S3).

For the calculation of the hygroscopicity parameter κ based on the measured aerosol chemical-composition data, we used the mass concentrations of OA, SO_4^{2-}, NO_3^-, NH_4^+ and Cl^- provided by ACSM. In this study, a simplified ion pairing scheme proposed by Gysel et al. (2007) was used to obtain the concentrations of AN, AS, ABS, and AC by turning mass concentrations of ions into mass concentrations of the corresponding inorganic salts. The κ values and densities of these salts are shown in Table S1 (Liu et al., 2014; Wu et al., 2016; Kuang et al., 2020). The simple mixing rule, called Zdanovsky-Stokes-Robinson (ZSR), is commonly used in κ_{chem} calculations, therefore, the κ_{chem} of this study can be calculated on the basis of chemical volume fractions ε_i (Petters and Kreidenweis, 2007) (see Text S4 for a detailed process).

3 Results and discussion

3.1 Overview of f(RH) and derived aerosol variables observations

The typical levels of light scattering coefficients (σ_{sp}), f(RH) values at RH = 80% (f(80%)), scattering Ångström exponents (α), $PM_{2.5}$ mass concentrations, and ambient RH from February to April 2022 were displayed in Figure S3. To evaluate the aerosol hygroscopicity conveniently, f(80%) was often employed (Xia et al., 2023; Xia et al., 2019; Zhao et al., 2019b; Wu et al., 2017). The scattering hygroscopic growth factor

f(80%) ranged from 1.00 to 2.48, with an average factor of 1.44 ± 0.15 during the whole campaign. The mean concentration of $PM_{2.5}$ was 24.79 ± 17.74 μg m^{-3}, suggested the $PM_{2.5}$ pollution was relative low in Xiamen referring to the air quality index (AQI) grading standard of China ($PM_{2.5}$ ⩽ 35 μg m^{-3}). During the period of observation, the hourly mean σ_{sp} measured under dry conditions varied from 1.15 to 662.57 Mm^{-1}, with a mean of 135.50 ± 108.78 Mm^{-1}, and its maximum occurred at the peak of $PM_{2.5}$ concentrations. The α was usually considered as an indicator of particle size, which was high when $PM_{2.5}$ level was low, indicating that there were more fine particles existed in $PM_{2.5}$ with low concentration. At the same time, the variation trend of *f*(80%) was similar to that of α. Ambient RH fluctuated considerably and was generally at a high level. The wind direction was more evenly distributed, and the wind speed was relatively stable, concentrated in 1-3 m/s. The comparison presented in Figure 1 and Table S2 implied that *f*(RH) varied widely across different regions, with consistently higher values observed in Europe compared to China. The differences between *f*(RH) in this study and in other regions of China were smaller than those outside of China. In urban China (Lin'an, Beijing, Guangzhou and Xiamen), *f*(RH) was generally small (Zhang et al., 2015; Zhao et al., 2019b; Ren et al., 2021; Li et al., 2021); whereas in Raoyang, greatly influenced by anthropogenic polluted aerosols, *f*(RH) raised significantly (Wu et al., 2017). Urban area in Europe (Granada, Spain) also displayed similar values of *f*(RH) (Titos et al., 2014). Nevertheless, the *f*(RH) of continental aerosols in Europe (Jungfraujoch, Swiss) obviously surpassed what had been observed in China (Zieger et al., 2013). In the Arctic (Ny- Ålesund, Svalbard) and the shore of the ocean (Mace Head), *f*(RH) showed high values due to the sea salt (Zieger et al., 2010; Zieger et al., 2013). However, Mace Head, which was also exposed to air pollution from the urban areas, had lower *f*(RH) than the undisturbed Arctic. Thus, the large variability of *f*(RH) across measurement sites was primarily attributed to the different aerosol sources and chemical composition.

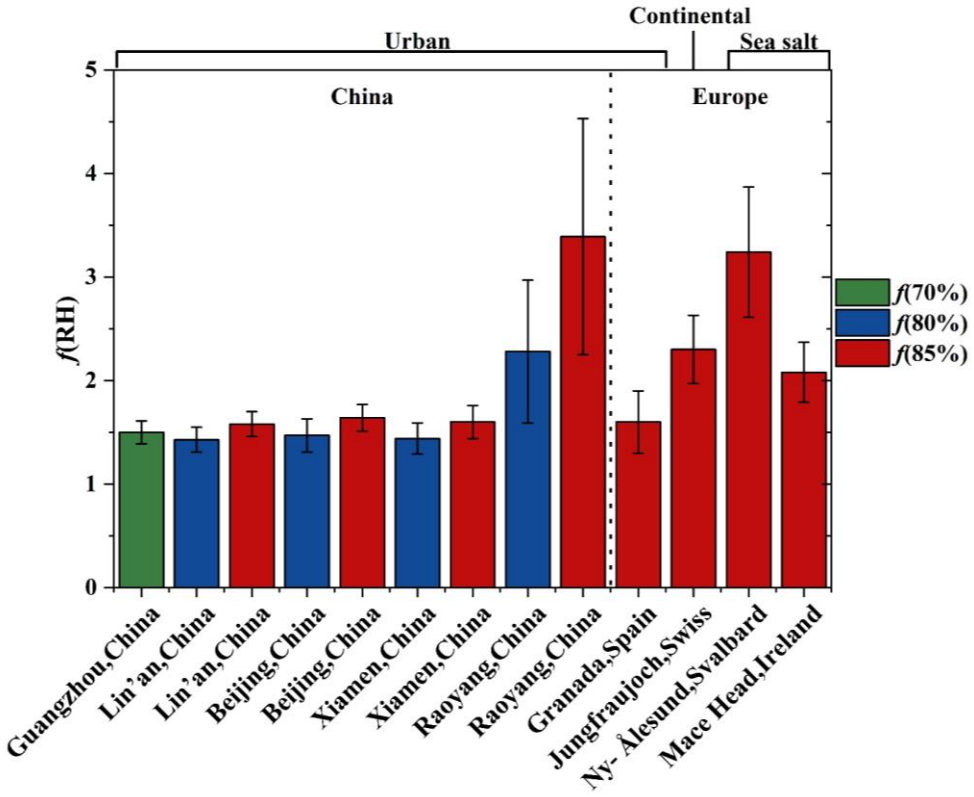

Figure 1. Mean values of *f*(80%), *f*(85%) and *f*(70%) values in different observation sites. The error bars represent standard deviation. Blue, green, and red represent *f*(80%), *f*(85%) and *f*(70%), respectively.

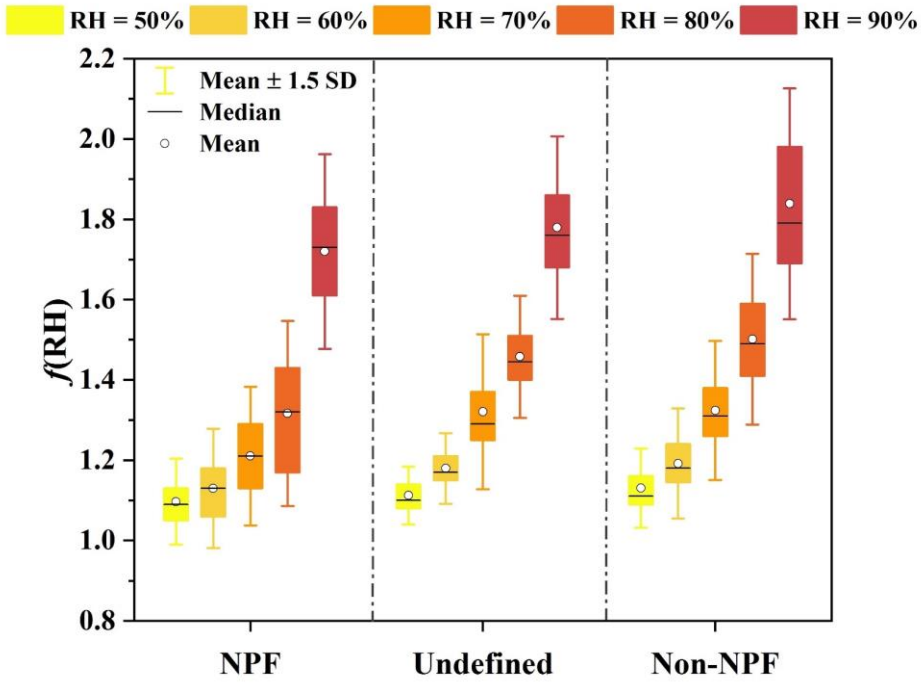

Figure 2. The *f*(RH) measured for a given RH in different days. The *f*(RH) values at RH=50%, 60%, 70%, 80%, and 90% were counted for the three types of days

NPF, Undefined, and non-NPF, respectively. Different colours represent different RH. The error bars represent the mean ± 1.5 standard deviation.

The entire campaign was devided into three type of days, NPF, Undefined, and non-NPF, based on the above classification method. The PNSD spectrum and number concentration of the example NPF and non-NPF days from February to April 2022 are shown in Figure S4 and Text S5. 11 NPF days were identified, representing approximately 12.94% of all observed days. In addition, we categorized 18 days as non-NPF days, and the remaining days as Undefinded. The statistical analysis of particle number concentrations in different days during the observation period was summarized in Table S3. The mean number concentration of nucleation, aitken and accumulation mode was $1.66 \times 10^3 \pm 1.59 \times 10^3$ cm^{-3}, $3.80 \times 10^3 \pm 2.80 \times 10^3$ cm^{-3} and $8.59 \times 10^2 \pm 4.04 \times 10^2$ cm^{-3} in NPF days, contributing 26.25%, 60.14% and 13.61% to total number concentration, respectively. The majority of particle number concentrations were comprised of nucleation and aitken mode particles. Figure 2 explores the variations of *f*(RH) with RH growth in different days. Firstly, *f*(RH) emerged an approximately exponential rise as RH increasing, with a significant growth when the RH ranged from 80% to 90%, the interval of which was the most beneficial to the aerosol scattering hygroscopic growth (Liu et al., 2013). Moreover, Zhao et al. (2019b) found a prominent difference in the aerosol hygroscopicity when RH exceeded 90%, with aerosol hygroscopicity in this humidity range being lower than when RH was below 90%. These results indicate that particles exhibited different hygroscopicity behaviors under different RH conditions, which were probably related to the chemical composition, particle size and morphology of aerosols. Secondly, the characteristics of *f*(RH) were distinct among different days, especially between NPF days and non-NPF days (Figure S5). When RH was below 80%, *f*(RH) was significantly lower during NPF days compared to non-NPF and Undefined days. The *f*(RH) growth of NPF days was greater than those of the other two sorts of days for RH between 80 and 90 %, and vice versa for RH below 80%. Such a growth pattern caused the *f*(RH) of the NPF days reaching a level equivalent to that of the other days as the RH rose to 90%. Moreover, the fluctuations of *f*(RH) were larger in the NPF days than in the other two sorts of days, indicating *f*(RH) in NPF days had a greater dispersion. These results might be related to the dramatic increase in particle number concentrations and variations in chemical composition during the NPF days.

The following discussion will focus on the differences in the aerosol scattering hygroscopic growth and the aerosol hygroscopicity between NPF and non-NPF. As Undefined days are in a transitional state, they do not accurately reflect the characteristics of the NPF.

3.2 Parameterization of the *f*(RH)

To better characterize the dependence of *f*(RH) on RH, many different empirical expressions have been applied in previous studies to fit the measurements of *f*(RH)

(Kotchenruther et al., 1999; Kotchenruther and Hobbs, 1998; Gasso et al., 2000; Carrico et al., 2003; Pan et al., 2009; Zieger et al., 2014; Yu et al., 2018). We fitted four commonly-used empirical equations to the *f*(RH) values, and compared the results to find that Eq. (2) (Chen et al., 2014) was the most suitable for describing the enhanced scattering caused by the monotonic hygroscopic growth (see Figure S6 and Text S6 for a detailed comparison).

$$f(\mathrm{RH}) = a\left(1 - \frac{RH}{100}\right)^{-b\left(\frac{\mathrm{RH}}{100}\right)} \quad (2)$$

where *a* is a coefficient that reflects the level of *f*(RH) values, and *b* is the parameter for the magnitude of scattering enhancement unaffected by RH that quantifies aerosol hygroscopicity to some extent. Higher *f*(RH) is related to higher "*a*" and "*b*" values.

The fitted *f*(RH) curves between NPF and non-NPF days over the entire observation period are presented in Figure 3. For these days, Eq.(2) was a difference in the fitting results, with fitting degrees being better in non-NPF days and relatively worse in NPF days. This reflects the fact that *f*(RH) on NPF days was influenced by more complex factors than on non-NPF days, including the source, composition, and morphology of the aerosols. The fitted *f*(RH) curve shown in Figure 3(a) is apparently below that shown in Figure 3(b). Similarly, both the observed *f*(80%) and the simulated *f*(80%) in the NPF days were lower compared to those in the non-NPF days. The *b* was lower for the NPF days, indicating that the aerosol hygroscopicity of the NPF days was weaker than those of non-NPF days. In this work, *b* was lower than that in the study done by Zhao et al. (2019b), but slightly higher than the findings of Chen et al. (2014) (Table S4), even though both of their studies were conducted in the North China Plain (NCP), where $PM_{2.5}$ concentrations and *f*(RH) were higher than those in Xiamen. Due to the proximity of *a*, a smaller *b* value resulted in the *f*(RH) being lower in this study compared to those in the NCP. It should be noted that the aerosol scattering hygroscopic growth does not necessarily weaken even in atmospheric environments with light particle pollution. This also shows that aerosol scattering hygroscopic growth is mainly controlled by the aerosol properties, such as aerosol chemical composition, etc., which are strongly related to the particle formation mechanism and the source of fine particles (Li et al., 2021; Chen et al., 2022a).

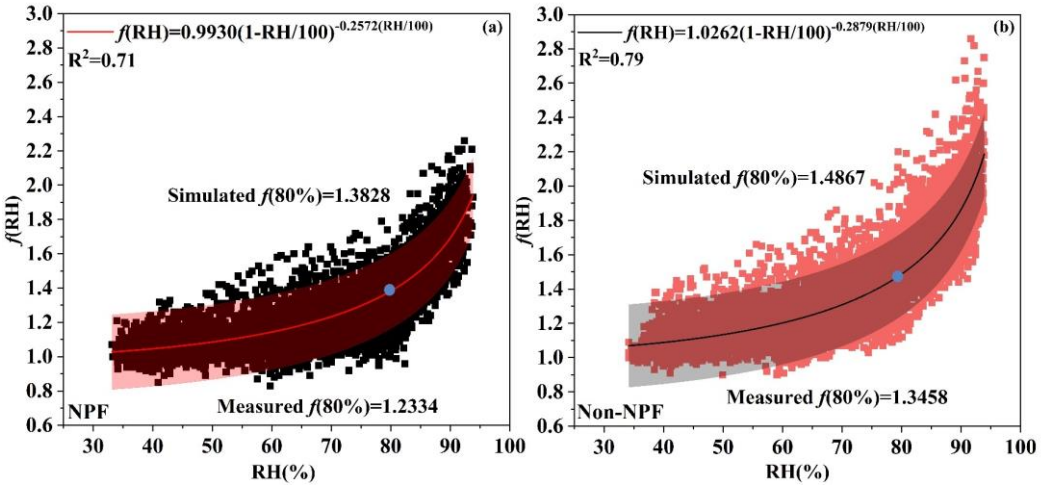

Figure 3. The *f*(RH) curves fitted by Eq.(2) on NPF and non-NPF days. (a) belongs to NPF days, (b) belongs to non-NPF days. Red and black lines are the curves fitted by Eq. (2), and blue dots represent the simulated values of *f*(80%). The light-color shaded areas show the 95 % prediction bands for the fits.

3.3 Distribution characteristics of *f*(RH) and aerosol chemical compositions

The mass concentration of the chemical components in NR-PM_1 (nonrefractory submicron particles), including SO_4, NO_3, NH_4, Chl and Org, and BC in aerosols were displayed in Table S5. SO_4, NO_3 and NH_4 (SNA) constituted the majority of the inorganic ions, which were converted from gaseous precursors by complex chemical processes in the atmosphere. Compared with ten years ago, the concentrations of all SNA in Xiamen have significantly decreased (Deng et al., 2016). The decline ratio in sulfate concentration reached 84.0%, indicating the effectiveness of sulfate control measures in recent years. In Xiamen, the main measures to control sulfate include the application of desulfurization technology in the flue gas of power plants and coal combustion boilers, as well as the promotion of clean energy for seaships. However, in contrast to the studies in 2011-2013 and 2017 (Wu et al., 2015a; Wu et al., 2020), the ratio of nitrate to sulfate had increased in this study, suggesting that nitrate pollution has become more prominent in recent years. The concentration of Org decreased in comparison to the previous study, while its proportion in aerosol remained unchanged (Chen et al., 2022b). Additionally, BC is regarded as hydrophobic species (Zieger et al., 2014).

The diurnal variation of *f*(80%) and chemical mass fractions are displayed in Figure 4. The diurnal variation of *f*(RH) was significantly related to the mass fraction of chemical components in particle. NPF days had an obvious lower values of *f*(80%) compared with the other event. The mass concentration of PM_1 in the non-NPF days (12.00 μg m^{-3}) was slightly lower than those in the NPF days (12.40 μg m^{-3}). The mass fraction of Org in the aerosol was higher during the NPF period than during the non-NPF period, and *f*(80%) in the NPF period was smaller than that in the non-NPF period. Based on the wind direction and the homology of Org with BC and CO (Figure S7, S8),

the increasing fraction of Org might be attributed to the emissions from heavy truck in the major roads near the observation site, which had a weaker impact on the aerosol hygroscopic growth than the SNA.

The *f*(80%) showed the same pattern as the mass fraction of SNA, especially for nitrate, and the amount of nitrate was significantly low during NPF period. The mass fraction of sulfate was much higher than that of nitrate on NPF days compared to non-NPF days. The SO_2 concentrations on NPF days were clearly higher than that on non-NPF days (Figure S9). Moreover, SO_2 concentrations increased from the morning and peaked around 15:00 on NPF days, which was consistent with the increasing trend of partice number concentration on NPF days. The reaction of SO_2 and OH radicals is considered as the primary pathway of sulfuric acid generation (Sipilä et al., 2010). Condensation mode reactions could occur due to the large amount of sulfuric acid in the atmosphere during NPF events. It is hypothesized that condensation mode reactions occurring simultaneously with NPF events were mainly responsible for the higher mass fraction of sulfate during NPF days observed at our site (Yue et al., 2010). Noted that the lower *f*(80%) in NPF period was probably attributed to the low mass fraction of nitrate and high mass fraction of sulfate in SNA. Chen et al. (2022a) reported that aerosol hygroscopic growth in Shanghai and Guangzhou during NPF days were lower than those during non-NPF days, which were consistent with the results of this study, but the opposite pattern occurred in the NCP. This illuminates that aerosols had a lower hygroscopicity during the NPF event in Xiamen. The study by Liu et al. (2021) also found that the hygroscopicity of 40 nm organic aerosol (OA) was significantly enhanced during NPF days in urban Beijing, which could be derived from different precursors and accounted for the formation of OA during the NPF process. On the basis of aerosol chemical compositions during NPF, it could be speculated that when particle formation occurs in NPF days, the condensation of large quantities of sulfuric acid and organic vapours onto the pre-existing particles results in the conversion of mixed state on the surface of particles from external mixture to internal mixture. These processes alter the optical and chemical properties of particles, which in turn might change the aerosol scattering hygroscopicity growth.(Wu et al., 2016)

The sulfur/nitrogen oxidation ratios (SOR/NOR) used to assess the extent of secondary sulphate and nitrate formation are shown in Figure 5, which were calculated from the formulas of $NOR=[NO_3]/([NO_3]+[NO_2])$ and $SOR=[SO_4]/([SO_4]+[SO_2])$, respectively (Liu et al., 2020b). The levels of SOR and NOR were subjected to the regulation by photochemical reactions, exhibiting an increase during daytime. Moreover, the variations in SOR/NOR levels and *f*(80%) across NPF days were found to be coincident, as SOR/NOR levels droped down, particularly for NOR, *f*(80%) also displayed a low level. We assume that nitrate was essential for aerosol scattering and hygroscopic growth. This assumption was confirmed by comparing Figure 4(a) (c) with Figure 5(a), which show a significant decline in *f*(RH) when both nitrate content and NOR were low, especially during NPF days. The sharp rise in NOR in the afternoon during the NPF days resulted in an significant increase in the relative amount of nitrate

in the aerosol and *f*(80%), indicating the rapid response of the aerosol hygroscopic growth to nitrate, which can be interpreted as a stronger hygroscopicity of nitrate compared to sulfate. In non-NPF days, SOR and NOR were enhanced compared to NPF days, which might be resulted from the aqueous phase reaction at relatively high RH (Sun et al., 2013; Ge et al., 2012). In non-NPF days with high RH and *f*(RH), water vapour condensed on the particles and aerosol hygroscopic growth occurred (Martin, 2000). The increase in aerosol liquid water content (ALWC) on the surface of particles is crucial for heterogeneous reactions in the atmosphere (Mogili et al., 2006). The heterogeneous hydrolysis of N_2O_5 (Pathak et al., 2009; Brown et al., 2005) and the aqueous-phase oxidation of SO_2 (Seinfeld et al., 1998; Sun et al., 2013) are important pathways for nitrate and sulfate formation, respectively. In other words, aqueous-phase reactions contribute to the production of secondary aerosol (Ge et al., 2012; Xu et al., 2017a). Thus, the elevation of RH during non-NPF days might promote the transformation of NO_2 and SO_2 to nitrate and sulfate via aqueous-phase reactions, manifesting as the enhancement of NOR and SOR.

In brief, the influence of SNA on *f*(RH), particularly nitrate, is significant. Sulfate dominated the SNA during the NPF days, characterized by weaker aerosol hygroscopic growth compared to non-NPF days, indicating the remarkably different bulk aerosol compositions and condensation mode of aerosol formation mechanisms between NPF and non-NPF days.

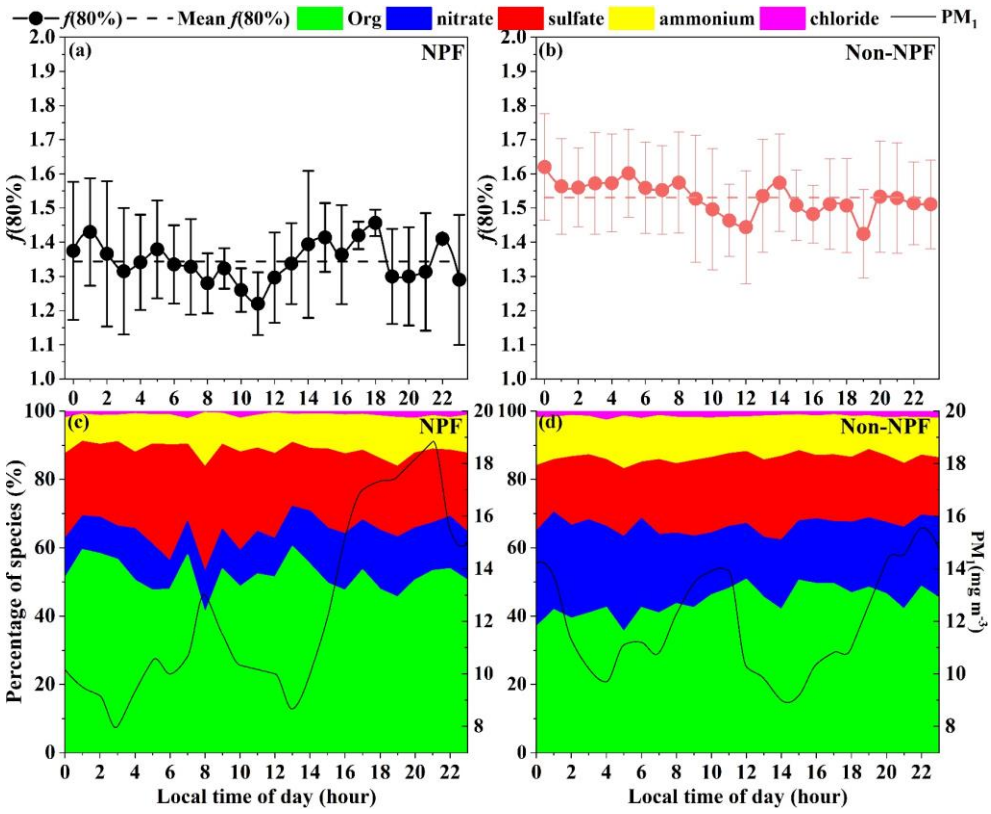

Figure 4. Diurnal variations of *f*(80%) and aerosol chemical mass fractions on NPF and non-NPF days. (a) and (c) belong to NPF days, (b) and (d) non-NPF days.

These chemical compositions include Org, NO_3, SO_4, NH_4, Chl. Solid lines are the mass concentrations of PM_1, dashed lines are the mean value of *f*(80%).

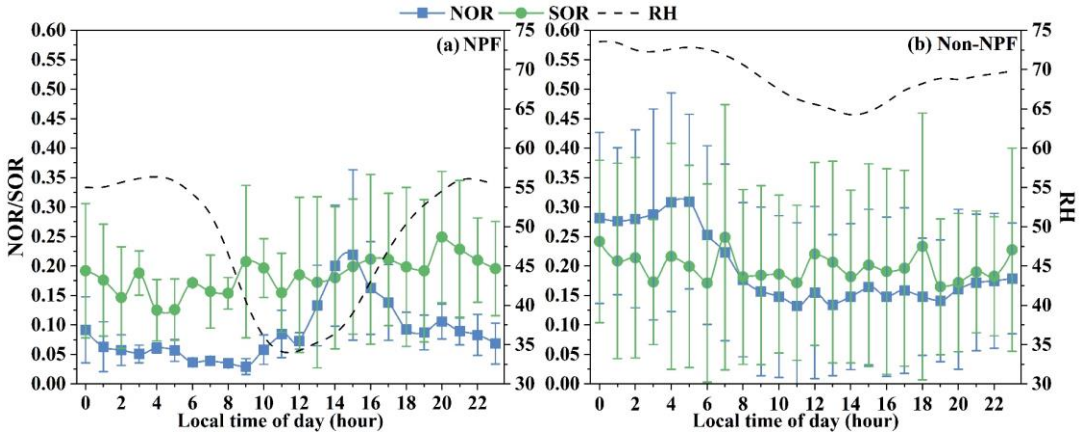

Figure 5. Diurnal variations of NOR, SOR and RH on NPF and non-NPF days. (a) belongs to NPF days, (b) belongs to non-NPF days. Blue represents NOR, green represents SOR, dashed lines are RH.

3.4 Relationships between *f*(RH) and aerosol chemical compositions

Figure 6 and Figure 7 exhibits *f*(80%) as a function of the mass fractions of SNA and Org between NPF and non-NPF days, revealing the effect of chemical compositions on the aerosol scattering hygroscopic growth. The SNA fraction showed a positive correlation with *f*(80%) as a result of its high hygroscopicity, whereas the Org fraction demonstrated a negative correlation with *f*(80%) due to its relative lower hygroscopicity compared to SNA, in line with findings from previous studies (Zhang et al., 2015; Wu et al., 2017; Ren et al., 2021; Zieger et al., 2014). The magnitude of R for the linear regression was higher during the NPF period compared to the non-NPF period, illuminating a stronger correlation between *f*(80%) and the mass fraction of SNA or Org specifically during NPF days. The proportion of aerosol chemical compositions remained relatively stable during the non-NPF days, which could be accounted for the limited correlation between *f*(80%) and their mass fractions during this period. Comparing Figure 6(a), 6(b) with Figure 7(a), 7(b), there was a stronger relationship between mass fraction of sulfate and *f*(80%) in NPF days. Conversely, a stronger association of *f*(80%) with nitrate was observed in non-NPF days. This indicated that sulfate had an important influence on the aerosol hygroscopicity enhancement during NPF period, while nitrate was the primary contributor for non-NPF days. This phenomenon could be explained by that the mass fraction of sulfate in the SNA was highest when the NPF event occurred, yet the differences between the mass fractions of sulfate and nitrate were slight in non-NPF days. The role of nitrate in the aerosol hygroscopic properties will be discussed in the following paragraphs.

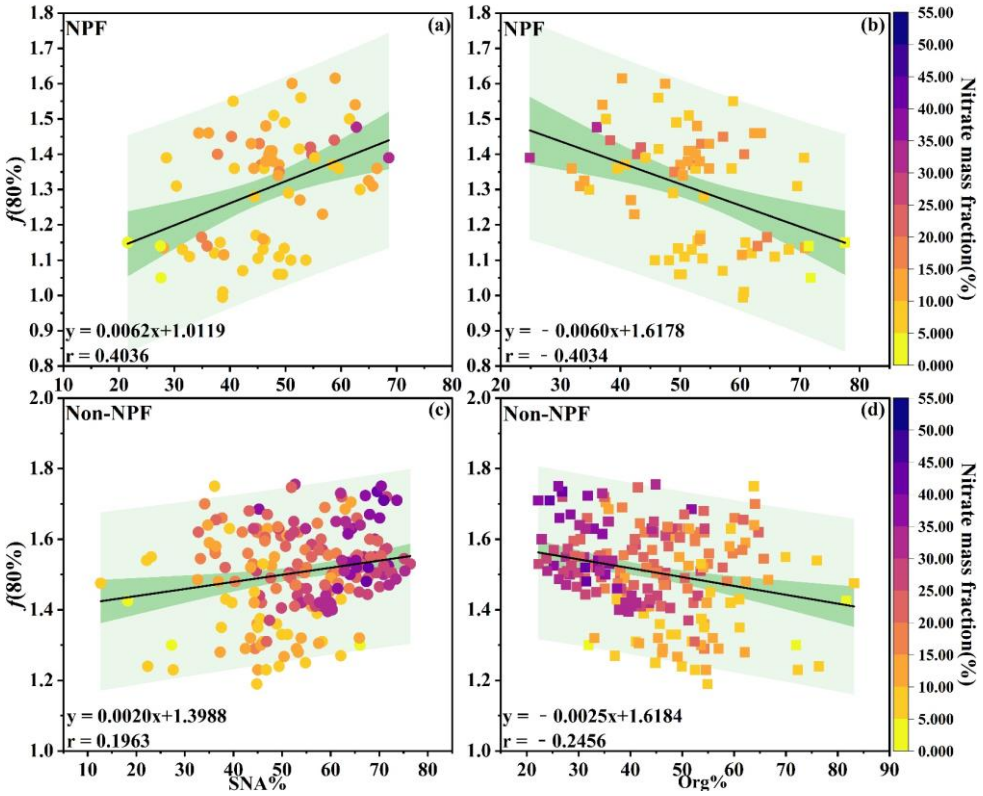

461

462 **Figure 6. The aerosol scattering hygroscopic growth factor *f*(80%) as a**
463 **function of SNA and Org mass fraction colored by the nitrate mass fraction.** (a)
464 and (b) belong to NPF days; (c) and (d) belong to non-NPF days. The linear regression
465 function and Pearson's correlation coefficient (R) are given in each panel. The dark-
466 color shaded areas denote 95 % confidence levels, and the light-color shaded areas
467 show the 95 % prediction bands for the fits.

468

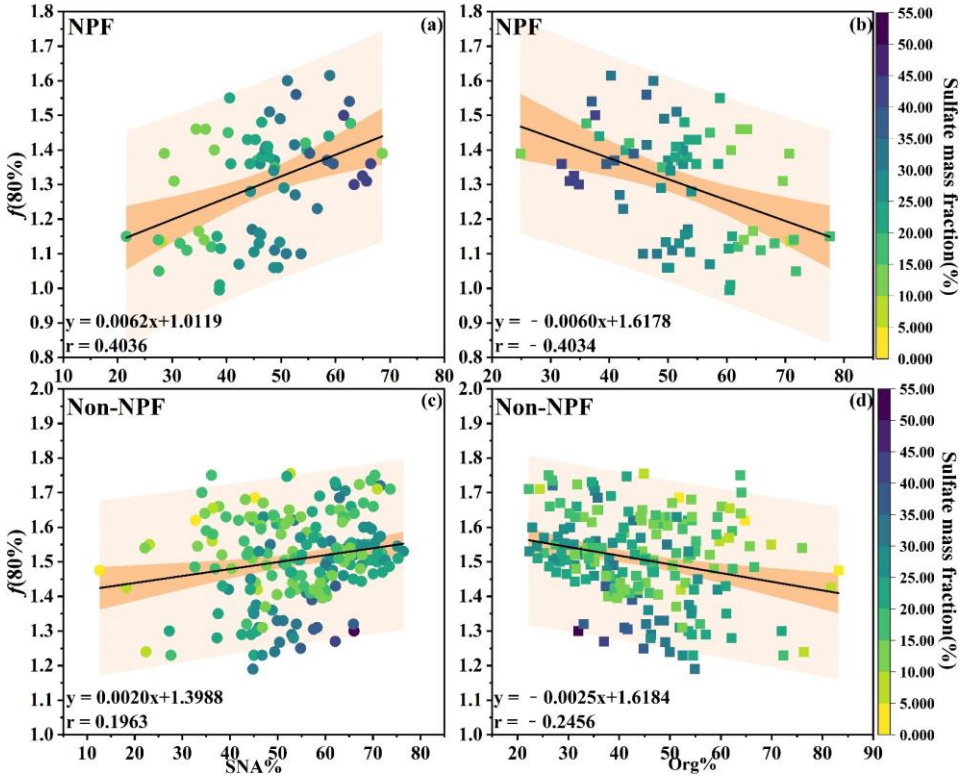

Figure 7. The aerosol scattering hygroscopic growth factor *f*(80%) as a function of SNA and Org mass fraction colored by the sulfate mass fraction. (a) and (b) belong to NPF days; (c) and (d) belong to non-NPF days. The linear regression function and Pearson's correlation coefficient (R) are given in each panel. The dark-color shaded areas denote 95 % confidence levels, and the light-color shaded areas show the 95 % prediction bands for the fits.

As mentioned above, the aerosol hygroscopic growth was significantly influenced by the proportion of SNA and Org in aerosols. The fitting parameter γ, which depends on the aerosol hygroscopicity, is defined as $\gamma = \ln f(RH)/\ln((100/RH_{ref})/(100-RH))$ (Quinn et al., 2005; Zhang et al., 2015). Here γ was based on RH_{ref} = 40 % and RH = 80 %. γ can be employed to characterize the relationship between aerosol hygroscopic growth and SNA. The relative quantity of Org and inorganic matters can be expressed as $F_o = Org/(Org + C_i)$, where C_i is the mass concentration of SNA. We chose NO_3, SO_4 and $NO_3 + SO_4$ as different SNA constitute in this study, respectively. γ and F_o were negatively correlated for all scatter plots, and linear regressions of γ versus F_o were fitted (Figure 8). γ and $F_O = Org/(Org + NO_3)$ (abbreviated as F_{O+N}, Figure 8a, d) were more strongly correlated than γ and $F_O = Org/(Org + SO_4)$ (abbreviated as F_{O+S}, Figure 8b, e). Additionally, the correlation between γ and $F_O = Org/(Org + NO_3 + SO_4)$ (abbreviated as F_{O+N+S}, Figure 8c, f) was observed to be smaller than that of the correlation between γ and F_{O+N}. This is yet more evidence that NO_3 played more important role than SO_4 in determining the aerosol hygroscopicity in Xiamen, contrary to the conclusion of Quinn et al. (2005), Malm et al. (2005) and Yan et al. (2009). This

findings also underscored the substantial impact of nitrate on aerosol properties, aligning with recent research conducted in various regions of China (Zhang et al., 2015; Sun et al., 2020; Liao et al., 2020; Jin et al., 2022).

Over the recent decades, the Chinese government has attached great importance to the air pollution control, and the prominent results have been achieved in reducing SO_2 emissions (Zhang et al., 2019; Zheng et al., 2018). As the concentration of SO_2 decreases, there might be an increasing trend for NH_3 to combine with NO_3^- to form NH_4NO_3, thereby enhancing the role of nitrate in atmospheric processes. The relative low value of *f*(80%) for NPF days can be explained by the fact that the organic and inorganic aerosol fractions were distinct, with sulfate being the predominant component of the inorganic aerosol during this period. During NPF days, there was a stronger correlation between γ and F_{O+S}, while the correlation of γ and F_{O+S} was extremely weak in non-NPF days, which could be related to the role of sulfuric acid in atmospheric nucleation in NPF days. Li et al. (2021) proposed the parameterization of γ according to its linear relationship beween F and TC, and the R^2 was 0.92, where, F was determined as the mass ratio of F= TC/(TC+ NO_3^- + SO_4^{2-}+ NH_4^+). However, the correlation between γ and F_{O+N+S} in this study was lower than that reported by Li et al. (2021). As the comparison with these parameterizations suggested, the comprehensive chemical composition information was likely in favor of accurate γ parameterizations and subsequent *f*(RH) determinations.

Overall, SNA are more effective in promoting aerosol hygroscopic growth than that of Org, with nitrate having the strongest impact.

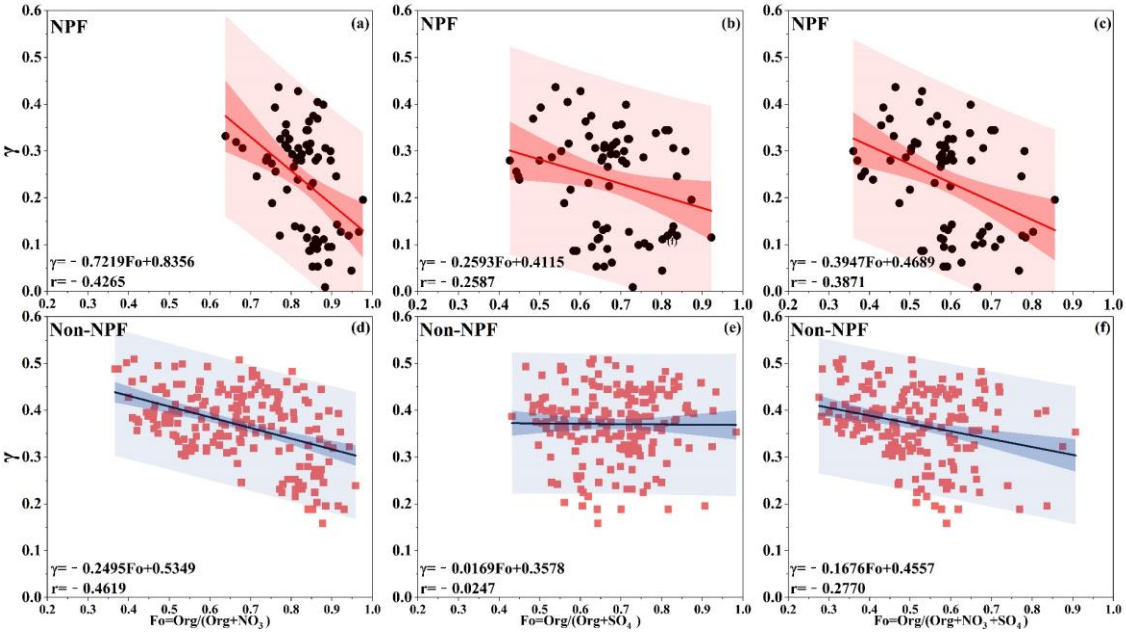

Figure 8. Scatter plots of γ versus the relative amount of Org and inorganics (F_o). (a, d) F_o= Org/(Org+ NO_3), (b, e) F_o = Org/(Org + SO_4), and (c, f) F_o= Org/(Org+ NO_3 + SO_4). (a), (b) and (c) belong to NPF event; (d), (e) and (f) belong to non-NPF event. Solid lines represent the linear fit. The dark-color shaded areas denote 95 %

confidence levels, and the light-color shaded areas show the 95 % prediction bands for the fits.

3.5 Aerosol hygroscopicity–chemical composition closure

The hygroscopicity parameter κ serves as a highly effective parameter for investigating aerosol hygroscopicity and can be assessed using the humidified nephelometer systems for aerosol light scattering hygroscopic growth factors. The $\kappa_{f(RH)}$, obtained from the measured aerosol scattering hygroscopic growth factor, is a function of the overall hygroscopicity of aerosol particles (Chen et al., 2014; Kuang et al., 2017; Kuang et al., 2020) and widely used to explain the influence of aerosol hygroscopic growth on aerosol optical properties (Tao et al., 2014; Kuang et al., 2015; Brock et al., 2016). Moreover, κ can be estimated based on the mass concentration and chemical composition of particles, commonly known as κ_{chem}. According to Kuang et al. (2020), $\kappa_{f(RH)}$ accurately represents κ_{chem} and can therefore be used for the aerosol hygroscopicity-chemistry composition closure, which was used to investigate the effect of aerosol chemical composition on the overall aerosol hygroscopicity in this study. The average $\kappa_{f(RH)}$ from 60% to 90% was used as a proxy for hygroscopicity closure.

Figure 9 shows the contribution of chemical composition to $\kappa_{f(RH)}$, calculated as the product of κ and its volume fraction for each aerosol chemical composition. During the observation period, the inorganic salts, especially SNA, played a major role in the aerosol hygroscopicity, while some previous studies found that low water-soluble compounds, most likely secondary organic species, predominantly promote new particle formation and have an effect on aerosol hygroscopicity and their cloud condensation nuclei (CCN) activity (Levin et al., 2012; Wu et al., 2015b; Väkevä et al., 2002). For aerosol hygroscopicity during NPF days, NH_4HSO_4 (ABS) was the most dominant contributor followed by NH_4NO_3 (AN). Although $(NH_4)_2SO_4$ (AS) ranked third place to aerosol hygroscopicity in NPF, it was still higher than its contributions to non-NPF days, which was consistent with the mentioned above that sulfate was the main factor influencing the aerosol scattering hygroscopicity growth during NPF period. The contribution of AN to aerosol hygroscopicity was predominant during non-NPF days, while the contribution of AS and ABS decreased substantially compared to those during NPF. The facilitation of organic aerosol (OA) to the aerosol hygroscopicity fluctuated considerably due to variations of OA composition under different events. The 26.57% of $\kappa_{f(RH)}$ attributed to OA in NPF was lower than that in non-NPF days. This phenomenon was probably associated with the variety of OA components, for instance, secondary organic aerosols (SOAs) exhibiting limited hygroscopicity(Wang et al., 2024). Furthermore, during non-NPF days, despite the increased contribution of OA to $\kappa_{f(RH)}$, f(RH) was higher than that of NPF days, which might be related to the increase in the overall aerosol hygroscopicity during this period and the change in physical properties of particles during these days (Wu et al., 2016).

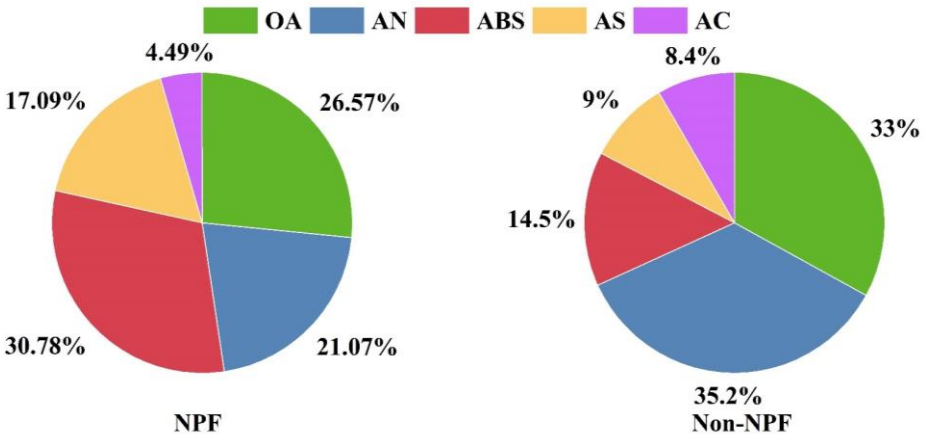

Figure 9. Contribution of aerosol chemical composition to $\kappa_{f(RH)}$ on NPF and non-NPF days. Green, blue, red, yellow, and purple code reprensent organic aerosol (OA), NH_4NO_3 (AN), NH_4HSO_4 (ABS), $(NH_4)_2SO_4$ (AS), and NH_4Cl (AC), respectively.

Due to the uncertainty in the hygroscopicity of OA, we investigated the characteristics of the hygroscopicity parameter κ_{OA} for organic aerosol, as well as the relationship between κ_{OA} and the oxidative properties of OA (Figure 10). Non-NPF days had the highest value of κ_{OA}, and NPF days had the lowest. The κ_{OA} values were greater than those of the previous study in China (Wu et al., 2016; Kuang et al., 2020; Kuang et al., 2021), but similar to the findings of Chang et al. (2010) at rural site in Ontario, Canada (Table 1). The proportion of POA and SOA in OA in our study (Figure S11) showed higher SOA mass fractions on non-NPF days than on NPF days. It is evident that high SOA mass fractions on non-NPF days corresponded to high κ_{OA} values. The results from these previous studies (Wu et al., 2016; Kuang et al., 2020; Kuang et al., 2021; Chang et al., 2010) also highlighted that SOA and oxygenated organic aerosols, were likely to be the determinants of κ_{OA}. Furthermore, SOA dominated OA mass both in this study and previous studies; however, κ_{OA} values differed much across studies. Noted that the hygroscopicity of SOA might vary significantly under different emission and atmospheric conditions due to variations in VOC precursors and SOA formation pathways (Kuang et al., 2021). The discrepantance in κ_{OA} suggests that using a constant κ_{OA} value to calculate κ might lead to a large bias.

Table 1. Comparisons of the average κ_{OA} in different study.

Study area	Periods	Remarks	Mean κ_{OA}	Reference
Beijing, China	Summer, 2014	urban	0.06	Wu et al. (2016)
Dingxing, China	2018/11/11-12/24	rural	0.08 ± 0.06	Kuang et al. (2020)
Heshan, China	2018/9/30-11/17	rural	0.085 ± 0.05	Kuang et al. (2021)

Ontario, Canada	Spring, 2007	rural	0.22 ± 0.04	Chang et al. (2010)
Xiamen, China	2022/2-4	urban	0.13 ± 0.11 (NPF) 0.19 ± 0.21 (non-NPF)	This study

To further investigate the factors affecting κ_{OA}, we compared the effect of OA oxidation level on κ_{OA}, where, f_{44} was used to represent the level of OA oxidation (Kuang et al., 2020; Chen et al., 2017). The values of f_{44} in the component mass spectrometry were ratio of *m/z* 44 to total signals, reflecting the absolute oxidation degree of aerosols (Chen et al., 2022b). The results showed a slightly weak correlation between κ_{OA} and the oxidation level of OA, indicating that the degree of oxidation was one of significant parameters in determining the hygroscopicity of OA. For both NPF days and non-NPF days, the hygroscopicity of OA enhanced with its oxidation level. Most of the previous studies on κ_{OA} had shown that the hygroscopicity of OA usually increased with the uplift of oxidation degree of OA, which was also found in this study. Nevertheless, a more pronounced increase in κ_{OA} with elevated f_{44} was observed in non-NPF days, attributing to the OA components, formation mechanisms, and the species of VOCs among diffenent events, which can also be accounted by the fact that less hygroscopic OA is produced during the NPF process in Xiamen, contrasted with the finding of Liu et al. (2021). Thereby, it could be found that alterations in the component and oxidation of OA might regulate the variation in κ_{OA} (Timonen et al., 2013; Xu et al., 2014; Xu et al., 2017b). In addition, the κ_{OA} values in NPF and non-NPF days were lower than those in the studies of Chen et al. (2017), Liu et al. (2021) and Kuang et al. (2020). These results reflect that the use of parameters related to oxidative properties, such as f_{44} or the ratio of O and C alone is not sufficient to characterize the hygroscopicity of OA, and that the molecular information of OA and the special formation mechanisms should also be considered (Liu et al., 2021). However, OA components is still one of the main driving force of the variation in aerosol hygroscopicity.

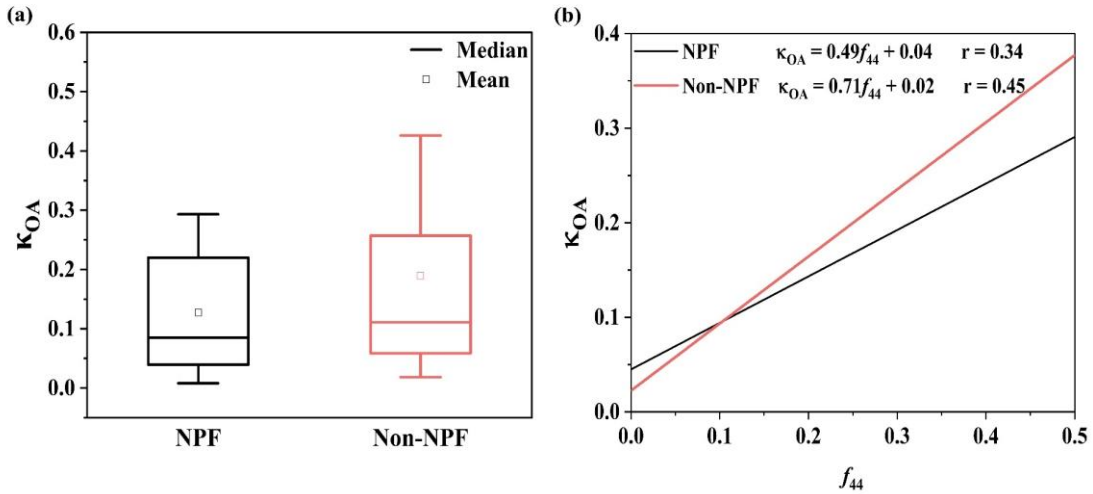

Figure 10. The derived κ_{OA} and f_{44} on NPF and non-NPF days. (a) Variation of κ_{OA} between NPF and non-NPF days. (b) The relationship between derived κ_{OA} and f_{44}.

4 Conclusions

In this study, the aerosol scattering hygroscopic growth during the new particle formation in Xiamen, the coastal city of southeast China, was clearly depicted by in situ observations. The distinct aerosol hygroscopic behaviors were evident during NPF events in the urban environment characterized by the elevated ambient temperatures, high levels of relative humidity, and low pollution. The aerosol scattering hygroscopic growth of NPF days was weaker than those of non-NPF days. However, under high RH conditions (80% to 90%), the f(RH) growth of NPF days exceeded that of non-NPF days. Furthermore, it was determined that one of the two-parameter fitting equations was more adept at accurately representing the observed f(RH).

The notable variations in f(RH) between NPF and non-NPF days were impacted by changes in SNA and Org of aerosols. SNA had a more important effect on f(RH) and a higher efficacy in enhancing aerosol hygroscopic growth than that of Org, with nitrate exhibiting the most pronounced impact. Sulfate was highlighted as the dominance in SNA during NPF days, with weaker f(RH) compared to non-NPF days. It is likely that the condensation mode reactions occurring simultaneously with NPF events changed the aerosol chemical composition and had an obvious effect on f(RH). The contribution of SNA to aerosol hygroscopicity surpassed that of Org, with ABS and AN dominating in NPF days and non-NPF days respectively, revealed by the aerosol hygroscopicity–chemical composition closure. The estimated κ_{OA} exhibited a decrease in NPF days compared to non-NPF days, and it showed an increase corresponding to the level of OA oxidation in both two types of days. The uncertainty in OA hygroscopicity resulted from variations in its components and oxidation states, however it was believed to be an important driver of the alteration in aerosol hygroscopicity. The findings in this study may provide a better explanation of aerosol hygroscopicity properties in the coastal city, which could also offer valuable insights into the use of hygroscopic growth factors in the models of air quality and climate change.

Data availability

The dataset for this paper can be accessed at https://doi.org/10.5281/zenodo.13756825 (Li et al., 2024).

Acknowledgements

This work was funded by the National Natural Science Foundation of China (U22A20578), the Science and Technology Department of Fujian Province (2022L3025), the National Key Research and Development Program (2022YFC3700304), STS Plan Supporting Project of the Chinese Academy of Sciences in Fujian Province (2023T3013), Fujian Provincial Environmental Protection Science & Technology Plan Projects (2023R004), Fujian Provincial Natural Science Foundation of China (2024J01199) and Xiamen Atmospheric Environment Observation and Research Station of Fujian Province.

Author contributions

ML and JC conceived the conceptual development of the paper. LL made measurements, analyzed the data and wrote the paper. ML designed the project and conducted the field campaigns. ML, XF and JC directed the manuscript development and editing. YC made measurements. All authors contributed to discussion and review.

Competing interests

The authors declare that they have no known competing financial interests or personal relationships that could have appeared to influence the work reported in this paper.

References

Baynard, T., Garland, R. M., Ravishankara, A. R., Tolbert, M. A., and Lovejoy, E. R.: Key factors influencing the relative humidity dependence of aerosol light scattering, Geophysical Research Letters, 33, 10.1029/2005gl024898, 2006.

Brock, C. A., Wagner, N. L., Anderson, B. E., Attwood, A. R., Beyersdorf, A., Campuzano-Jost, P., Carlton, A. G., Day, D. A., Diskin, G. S., Gordon, T. D., Jimenez, J. L., Lack, D. A., Liao, J., Markovic, M. Z., Middlebrook, A. M., Ng, N. L., Perring, A. E., Richardson, M. S., Schwarz, J. P., Washenfelder, R. A., Welti, A., Xu, L., Ziemba, L. D., and Murphy, D. M.: Aerosol optical properties in the southeastern United States in summer - Part 1: Hygroscopic growth, Atmospheric Chemistry and Physics, 16, 4987-5007, 10.5194/acp-16-4987-2016, 2016.

Brown, S. S., Osthoff, H. D., Stark, H., Dubé, W. P., Ryerson, T. B., Warneke, C., de Gouw, J. A., Wollny, A. G., Parrish, D. D., Fehsenfeld, F. C., and Ravishankara, A. R.: Aircraft observations of daytime NO3 and N2O5 and their implications for tropospheric chemistry, Journal of Photochemistry and Photobiology a-Chemistry, 176, 270-278, 10.1016/j.jphotochem.2005.10.004, 2005.

Carrico, C. M., Kus, P., Rood, M. J., Quinn, P. K., and Bates, T. S.: Mixtures of pollution, dust, sea salt, and volcanic aerosol during ACE-Asia: Radiative properties as a function of relative humidity, Journal of Geophysical Research-Atmospheres, 108, 10.1029/2003jd003405, 2003.

Chang, R. Y. W., Slowik, J. G., Shantz, N. C., Vlasenko, A., Liggio, J., Sjostedt, S. J., Leaitch, W. R., and Abbatt, J. P. D.: The hygroscopicity parameter (κ) of ambient organic aerosol at a field site subject to biogenic and anthropogenic influences: relationship to degree of aerosol oxidation, Atmospheric Chemistry and Physics, 10, 5047-5064, 10.5194/acp-10-5047-2010, 2010.

Charlson, R. J., Schwartz, S. E., Hales, J. M., Cess, R. D., Coakley, J. A., Hansen, J. E., and Hofmann, D. J.: Climate Forcing By Anthropogenic Aerosols, Science, 255, 423-430, 10.1126/science.255.5043.423, 1992.

Chen, G. J., Shi, Q., Xu, L. L., Yu, S. C., Lin, Z. Y., Ji, X. T., Fan, X. L., Hong, Y. W., Li, M. R., Zhang, F. W., Chen, J. F., and Chen, J. S.: Photochemistry in the urban agglomeration along the coastline of southeastern China: Pollution mechanism and control implication, Science of the Total Environment, 901, 10.1016/j.scitotenv.2023.166318, 2023.

Chen, J., Zhao, C. S., Ma, N., and Yan, P.: Aerosol hygroscopicity parameter derived from the light scattering enhancement factor measurements in the North China Plain, Atmospheric Chemistry and Physics, 14, 8105-8118, 10.5194/acp-14-8105-2014, 2014.

Chen, J., Budisulistiorini, S. H., Itoh, M., Lee, W. C., Miyakawa, T., Komazaki, Y., Yang, L. D. Q., and Kuwata, M.: Water uptake by fresh Indonesian peat burning particles is limited by water-soluble organic matter, Atmospheric Chemistry and Physics, 17, 11591-11604, 10.5194/acp-17-11591-2017, 2017.

Chen, L., Zhang, F., Zhang, D. M., Wang, X. M., Song, W., Liu, J. Y., Ren, J. Y., Jiang, S. H., Li, X., and Li, Z. Q.: Measurement report: Hygroscopic growth of ambient fine

711 particles measured at five sites in China, Atmospheric Chemistry and Physics, 22, 6773-
712 6786, 10.5194/acp-22-6773-2022, 2022a.
713 Chen, T. Z., Chu, B. W., Ma, Q. X., Zhang, P., Liu, J., and He, H.: Effect of relative
714 humidity on SOA formation from aromatic hydrocarbons: Implications from the
715 evolution of gas- and particle -phase species, Science of the Total Environment, 773,
716 10.1016/j.scitotenv.2021.145015, 2021.
717 Chen, Y. P., Yang, C., Xu, L. L., Chen, J. S., Zhang, Y. R., Shi, J. Y., Fan, X. L., Zheng,
718 R. H., Hong, Y. W., and Li, M. R.: Chemical composition of NR-PM1 in a coastal city
719 of Southeast China: Temporal variations and formation pathways, Atmospheric
720 Environment, 285, 10.1016/j.atmosenv.2022.119243, 2022b.
721 Covert, D. S., Charlson, R. J., and Ahlquist, N. C.: A Study of the Relationship of
722 Chemical Composition and Humidity to Light Scattering by Aerosols, Journal of
723 Applied Meteorology and Climatology, 11, 968-976, https://doi.org/10.1175/1520-
724 0450(1972)011<0968:ASOTRO>2.0.CO;2, 1972.
725 Dal Maso, M., Kulmala, M., Riipinen, I., Wagner, R., Hussein, T., Aalto, P. P., and
726 Lehtinen, K. E. J.: Formation and growth of fresh atmospheric aerosols: eight years of
727 aerosol size distribution data from SMEAR II, Hyytiala, Finland, Boreal Environment
728 Research, 10, 323-336, 2005.
729 Deng, J. J., Zhang, Y. R., Hong, Y. W., Xu, L. L., Chen, Y. T., Du, W. J., and Chen, J.
730 S.: Optical properties of PM2.5 and the impacts of chemical compositions in the coastal
731 city Xiamen in China, Science of the Total Environment, 557, 665-675,
732 10.1016/j.scitotenv.2016.03.143, 2016.
733 Ding, J., Zhang, Y., Zheng, N., Zhang, H., Yu, Z., Li, L., Yuan, J., Tang, M., and Feng,
734 Y.: Size Distribution of Aerosol Hygroscopic Growth Factors in Winter in Tianjin,
735 Environmental Science, 42, 574-583, 2021.
736 Duplissy, J., DeCarlo, P. F., Dommen, J., Alfarra, M. R., Metzger, A., Barmpadimos, I.,
737 Prevot, A. S. H., Weingartner, E., Tritscher, T., Gysel, M., Aiken, A. C., Jimenez, J. L.,
738 Canagaratna, M. R., Worsnop, D. R., Collins, D. R., Tomlinson, J., and Baltensperger,
739 U.: Relating hygroscopicity and composition of organic aerosol particulate matter,
740 Atmospheric Chemistry and Physics, 11, 1155-1165, 10.5194/acp-11-1155-2011, 2011.
741 Fierz-Schmidhauser, R., Zieger, P., Vaishya, A., Monahan, C., Bialek, J., O'Dowd, C.
742 D., Jennings, S. G., Baltensperger, U., and Weingartner, E.: Light scattering
743 enhancement factors in the marine boundary layer (Mace Head, Ireland), Journal of
744 Geophysical Research-Atmospheres, 115, 10.1029/2009jd013755, 2010a.
745 Fierz-Schmidhauser, R., Zieger, P., Wehrle, G., Jefferson, A., Ogren, J. A.,
746 Baltensperger, U., and Weingartner, E.: Measurement of relative humidity dependent
747 light scattering of aerosols, Atmospheric Measurement Techniques, 3, 39-50,
748 10.5194/amt-3-39-2010, 2010b.
749 Gasso, S., Hegg, D. A., Covert, D. S., Collins, D., Noone, K. J., Ostrom, E., Schmid,
750 B., Russell, P. B., Livingston, J. M., Durkee, P. A., and Jonsson, H.: Influence of
751 humidity on the aerosol scattering coefficient and its effect on the upwelling radiance
752 during ACE-2, Tellus Series B-Chemical and Physical Meteorology, 52, 546-567,

753 10.1034/j.1600-0889.2000.00055.x, 2000.
754 Ge, X. L., Zhang, Q., Sun, Y. L., Ruehl, C. R., and Setyan, A.: Effect of aqueous-phase
755 processing on aerosol chemistry and size distributions in Fresno, California, during
756 wintertime, Environmental Chemistry, 9, 221-235, 10.1071/en11168, 2012.
757 Giordano, M., Espinoza, C., and Asa-Awuku, A.: Experimentally measured
758 morphology of biomass burning aerosol and its impacts on CCN ability, Atmospheric
759 Chemistry and Physics, 15, 1807-1821, 10.5194/acp-15-1807-2015, 2015.
760 Guan, X., Wang, M., Du, T., Tian, P. F., Zhang, N. Y., Shi, J. S., Chang, Y., Zhang, L.,
761 Zhang, M., Song, X., and Sun, Y. J.: Wintertime aerosol optical properties in Lanzhou,
762 Northwest China: Emphasis on the rapid increase of aerosol absorption under high
763 particulate pollution, Atmospheric Environment, 246,
764 10.1016/j.atmosenv.2020.118081, 2021.
765 Gysel, M., Crosier, J., Topping, D. O., Whitehead, J. D., Bower, K. N., Cubison, M. J.,
766 Williams, P. I., Flynn, M. J., McFiggans, G. B., and Coe, H.: Closure study between
767 chemical composition and hygroscopic growth of aerosol particles during TORCH2,
768 Atmospheric Chemistry and Physics, 7, 6131-6144, 10.5194/acp-7-6131-2007, 2007.
769 Holmes, N. S.: A review of particle formation events and growth in the atmosphere in
770 the various environments and discussion of mechanistic implications, Atmospheric
771 Environment, 41, 2183-2201, 10.1016/j.atmosenv.2006.10.058, 2007.
772 IPCC: Climate Change 2021: The Physical Science Basis. Contribution of Working
773 Group I to the Sixth Assessment Report of the Intergovernmental Panel on Climate
774 Change, Cambridge University Press, In Press, 2021.
775 Jin, X. A., Li, Z. Q., Wu, T., Wang, Y. Y., Su, T. N., Ren, R. M., Wu, H., Zhang, D. M.,
776 Li, S. Z., and Cribb, M.: Differentiating the Contributions of Particle Concentration,
777 Humidity, and Hygroscopicity to Aerosol Light Scattering at Three Sites in China,
778 Journal of Geophysical Research-Atmospheres, 127, 10.1029/2022jd036891, 2022.
779 Kalkavouras, P., BougiatiotI, A., Hussein, T., Kalivitis, N., Stavroulas, I.,
780 Michalopoulos, P., and Mihalopoulos, N.: Regional New Particle Formation over the
781 Eastern Mediterranean and Middle East, Atmosphere, 12, 10.3390/atmos12010013,
782 2021.
783 Kotchenruther, R. A., and Hobbs, P. V.: Humidification factors of aerosols from biomass
784 burning in Brazil, Journal of Geophysical Research-Atmospheres, 103, 32081-32089,
785 10.1029/98jd00340, 1998.
786 Kotchenruther, R. A., Hobbs, P. V., and Hegg, D. A.: Humidification factors for
787 atmospheric aerosols off the mid-Atlantic coast of the United States, Journal of
788 Geophysical Research-Atmospheres, 104, 2239-2251, 10.1029/98jd01751, 1999.
789 Kreidenweis, S. M., and Asa-Awuku, A.: Aerosol Hygroscopicity: Particle Water
790 Content and Its Role in Atmospheric Processes, Treatise on Geochemistry, 5, 331-361,
791 2014.
792 Kuang, Y., Zhao, C. S., Tao, J. C., and Ma, N.: Diurnal variations of aerosol optical
793 properties in the North China Plain and their influences on the estimates of direct
794 aerosol radiative effect, Atmospheric Chemistry and Physics, 15, 5761-5772,

10.5194/acp-15-5761-2015, 2015.
Kuang, Y., Zhao, C. S., Tao, J. C., Bian, Y. X., Ma, N., and Zhao, G.: A novel method for deriving the aerosol hygroscopicity parameter based only on measurements from a humidified nephelometer system, Atmospheric Chemistry and Physics, 17, 6651-6662, 10.5194/acp-17-6651-2017, 2017.
Kuang, Y., He, Y., Xu, W. Y., Zhao, P. S., Cheng, Y. F., Zhao, G., Tao, J. C., Ma, N., Su, H., Zhang, Y. Y., Sun, J. Y., Cheng, P., Yang, W. D., Zhang, S. B., Wu, C., Sun, Y. L., and Zhao, C. S.: Distinct diurnal variation in organic aerosol hygroscopicity and its relationship with oxygenated organic aerosol, Atmospheric Chemistry and Physics, 20, 865-880, 10.5194/acp-20-865-2020, 2020.
Kuang, Y., Huang, S., Xue, B. A., Luo, B. A., Song, Q. C., Chen, W., Hu, W. W., Li, W., Zhao, P. S., Cai, M. F., Peng, Y. W., Qi, J. P., Li, T. G., Wang, S. H., Chen, D. H., Yue, D. L., Yuan, B., and Shao, M.: Contrasting effects of secondary organic aerosol formations on organic aerosol hygroscopicity, Atmospheric Chemistry and Physics, 21, 10375-10391, 10.5194/acp-21-10375-2021, 2021.
Kulmala, M., Petaja, T., Nieminen, T., Sipila, M., Manninen, H. E., Lehtipalo, K., Dal Maso, M., Aalto, P. P., Junninen, H., Paasonen, P., Riipinen, I., Lehtinen, K. E. J., Laaksonen, A., and Kerminen, V. M.: Measurement of the nucleation of atmospheric aerosol particles, Nature Protocols, 7, 1651-1667, 10.1038/nprot.2012.091, 2012.
Levin, E. J. T., Prenni, A. J., Petters, M. D., Kreidenweis, S. M., Sullivan, R. C., Atwood, S. A., Ortega, J., DeMott, P. J., and Smith, J. N.: An annual cycle of size-resolved aerosol hygroscopicity at a forested site in Colorado, Journal of Geophysical Research-Atmospheres, 117, 10.1029/2011jd016854, 2012.
Li, J. W., Zhang, Z. S., Wu, Y. F., Tao, J., Xia, Y. J., Wang, C. Y., and Zhang, R. J.: Effects of chemical compositions in fine particles and their identified sources on hygroscopic growth factor during dry season in urban Guangzhou of South China, Science of the Total Environment, 801, 10.1016/j.scitotenv.2021.149749, 2021.
Liao, W. J., Zhou, J. B., Zhu, S. J., Xiao, A. S., Li, K., and Schauer, J. J.: Characterization of aerosol chemical composition and the reconstruction of light extinction coefficients during winter in Wuhan, China, Chemosphere, 241, 10.1016/j.chemosphere.2019.125033, 2020.
Liu, H. J., Zhao, C. S., Nekat, B., Ma, N., Wiedensohler, A., van Pinxteren, D., Spindler, G., Muller, K., and Herrmann, H.: Aerosol hygroscopicity derived from size-segregated chemical composition and its parameterization in the North China Plain, Atmospheric Chemistry and Physics, 14, 2525-2539, 10.5194/acp-14-2525-2014, 2014.
Liu, J. Y., Ren, C. H., Huang, X., Nie, W., Wang, J. P., Sun, P., Chi, X. G., and Ding, A. J.: Increased Aerosol Extinction Efficiency Hinders Visibility Improvement in Eastern China, Geophysical Research Letters, 47, 10.1029/2020gl090167, 2020a.
Liu, J. Y., Zhang, F., Xu, W. Q., Sun, Y. L., Chen, L., Li, S. Z., Ren, J. Y., Hu, B., Wu, H., and Zhang, R. Y.: Hygroscopicity of Organic Aerosols Linked to Formation Mechanisms, Geophysical Research Letters, 48, 10.1029/2020gl091683, 2021.
Liu, T. T., Hu, B. Y., Yang, Y. X., Li, M. R., Hong, Y. W., Xu, X. B., Xu, L. L., Chen,

N. H., Chen, Y. T., Xiao, H., and Chen, J. S.: Characteristics and source apportionment of PM2.5 on an island in Southeast China: Impact of sea-salt and monsoon, Atmospheric Research, 235, 10.1016/j.atmosres.2019.104786, 2020b.
Liu, T. T., Hong, Y. W., Li, M. R., Xu, L. L., Chen, J. S., Bian, Y. H., Yang, C., Dan, Y. B., Zhang, Y. N., Xue, L. K., Zhao, M., Huang, Z., and Wang, H.: Atmospheric oxidation capacity and ozone pollution mechanism in a coastal city of southeastern China: analysis of a typical photochemical episode by an observation-based model, Atmospheric Chemistry and Physics, 22, 2173-2190, 10.5194/acp-22-2173-2022, 2022.
Liu, X., and Zhang, Y.: Advances in Research on Aerosol Hygroscopic Properties at Home and Abroad, Climatic and Environmental Research, 15, 808-816, 2010.
Liu, X. G., Zhang, Y. H., Cheng, Y. F., Hu, M., and Han, T. T.: Aerosol hygroscopicity and its impact on atmospheric visibility and radiative forcing in Guangzhou during the 2006 PRIDE-PRD campaign, Atmospheric Environment, 60, 59-67, 10.1016/j.atmosenv.2012.06.016, 2012.
Liu, X. G., Gu, J. W., Li, Y. P., Cheng, Y. F., Qu, Y., Han, T. T., Wang, J. L., Tian, H. Z., Chen, J., and Zhang, Y. H.: Increase of aerosol scattering by hygroscopic growth: Observation, modeling, and implications on visibility, Atmospheric Research, 132, 91-101, 10.1016/j.atmosres.2013.04.007, 2013.
Malm, W. C., and Day, D. E.: Estimates of aerosol species scattering characteristics as a function of relative humidity, Atmospheric Environment, 35, 2845-2860, 10.1016/s1352-2310(01)00077-2, 2001.
Malm, W. C., Day, D. E., Kreidenweis, S. M., Collett, J. L., Carrico, C., McMeeking, G., and Lee, T.: Hygroscopic properties of an organic-laden aerosol, Atmospheric Environment, 39, 4969-4982, 10.1016/j.atmosenv.2005.05.014, 2005.
Martin, S. T.: Phase Transitions of Aqueous Atmospheric Particles, Chemical Reviews, 100, 3403-3454, 10.1021/cr990034t, 2000.
Mogili, P. K., Kleiber, P. D., Young, M. A., and Grassian, V. H.: N2O5 hydrolysis on the components of mineral dust and sea salt aerosol:: Comparison study in an environmental aerosol reaction chamber, Atmospheric Environment, 40, 7401-7408, 10.1016/j.atmosenv.2006.06.048, 2006.
Pan, X. L., Yan, P., Tang, J., Ma, J. Z., Wang, Z. F., Gbaguidi, A., and Sun, Y. L.: Observational study of influence of aerosol hygroscopic growth on scattering coefficient over rural area near Beijing mega-city, Atmospheric Chemistry and Physics, 9, 7519-7530, 10.5194/acp-9-7519-2009, 2009.
Pathak, R. K., Wu, W. S., and Wang, T.: Summertime PM2.5 ionic species in four major cities of China: nitrate formation in an ammonia-deficient atmosphere, Atmospheric Chemistry and Physics, 9, 1711-1722, 10.5194/acp-9-1711-2009, 2009.
Petters, M. D., and Kreidenweis, S. M.: A single parameter representation of hygroscopic growth and cloud condensation nucleus activity, Atmospheric Chemistry and Physics, 7, 1961-1971, 10.5194/acp-7-1961-2007, 2007.
Quinn, P. K., Bates, T. S., Baynard, T., Clarke, A. D., Onasch, T. B., Wang, W., Rood, M. J., Andrews, E., Allan, J., Carrico, C. M., Coffman, D., and Worsnop, D.: Impact of

particulate organic matter on the relative humidity dependence of light scattering: A simplified parameterization, Geophysical Research Letters, 32, 10.1029/2005gl024322, 2005.
Ren, R. M., Li, Z. Q., Yan, P., Wang, Y. Y., Wu, H., Cribb, M., Wang, W., Jin, X. A., Li, Y. A., and Zhang, D. M.: Measurement report: The effect of aerosol chemical composition on light scattering due to the hygroscopic swelling effect, Atmospheric Chemistry and Physics, 21, 9977-9994, 10.5194/acp-21-9977-2021, 2021.
Seinfeld, J., Pandis, S., and Noone, K.: Atmospheric Chemistry and Physics: From Air Pollution to Climate Change, Physics Today, 51, 88-90, 1998.
Shen, X. J., Sun, J. Y., Ma, Q. L., Zhang, Y. M., Zhong, J. T., Yue, Y., Xia, C., Hu, X. Y., Zhang, S. N., and Zhang, X. Y.: Long-term trend of new particle formation events in the Yangtze River Delta, China and its influencing factors: 7-year dataset analysis, Science of the Total Environment, 807, 10.1016/j.scitotenv.2021.150783, 2022.
Sheridan, P. J., Delene, D. J., and Ogren, J. A.: Four years of continuous surface aerosol measurements from the Department of Energy's Atmospheric Radiation Measurement Program Southern Great Plains Cloud and Radiation Testbed site, Journal of Geophysical Research-Atmospheres, 106, 20735-20747, 10.1029/2001jd000785, 2001.
Sheridan, P. J., Jefferson, A., and Ogren, J. A.: Spatial variability of submicrometer aerosol radiative properties over the Indian Ocean during INDOEX, Journal of Geophysical Research-Atmospheres, 107, 10.1029/2000jd000166, 2002.
Sipilä, M., Berndt, T., Petäjä, T., Brus, D., Vanhanen, J., Stratmann, F., Patokoski, J., Mauldin, R. L., Hyvärinen, A. P., Lihavainen, H., and Kulmala, M.: The Role of Sulfuric Acid in Atmospheric Nucleation, Science, 327, 1243-1246, 10.1126/science.1180315, 2010.
Stevens, R., and Dastoor, A.: A Review of the Representation of Aerosol Mixing State in Atmospheric Models, Atmosphere, 10, 10.3390/atmos10040168, 2019.
Sun, P., Nie, W., Wang, T. Y., Chi, X. G., Huang, X., Xu, Z., Zhu, C. J., Wang, L., Qi, X. M., Zhang, Q., and Ding, A. J.: Impact of air transport and secondary formation on haze pollution in the Yangtze River Delta: In situ online observations in Shanghai and Nanjing, Atmospheric Environment, 225, 10.1016/j.atmosenv.2020.117350, 2020.
Sun, Y. L., Wang, Z. F., Fu, P. Q., Jiang, Q., Yang, T., Li, J., and Ge, X. L.: The impact of relative humidity on aerosol composition and evolution processes during wintertime in Beijing, China, Atmospheric Environment, 77, 927-934, 10.1016/j.atmosenv.2013.06.019, 2013.
Tang, I. N.: Chemical and size effects of hygroscopic aerosols on light scattering coefficients, Journal of Geophysical Research-Atmospheres, 101, 19245-19250, 10.1029/96jd03003, 1996.
Tao, J. C., Zhao, C. S., Ma, N., and Liu, P. F.: The impact of aerosol hygroscopic growth on the single-scattering albedo and its application on the NO₂ photolysis rate coefficient, Atmospheric Chemistry and Physics, 14, 12055-12067, 10.5194/acp-14-12055-2014, 2014.
Timonen, H., Carbone, S., Aurela, M., Saarnio, K., Saarikoski, S., Ng, N. L.,

Canagaratna, M. R., Kulmala, M., Kerminen, V. M., Worsnop, D. R., and Hillamo, R.: Characteristics, sources and water-solubility of ambient submicron organic aerosol in springtime in Helsinki, Finland, Journal of Aerosol Science, 56, 61-77, 10.1016/j.jaerosci.2012.06.005, 2013.
Titos, G., Lyamani, H., Cazorla, A., Sorribas, M., Foyo-Moreno, I., Wiedensohler, A., and Alados-Arboledas, L.: Study of the relative humidity dependence of aerosol light-scattering in southern Spain, Tellus Series B-Chemical and Physical Meteorology, 66, 10.3402/tellusb.v66.24536, 2014.
Väkevä, M., Hämeri, K., and Aalto, P. P.: Hygroscopic properties of nucleation mode and Aitken mode particles during nucleation bursts and in background air -: art. no. 8104, Journal of Geophysical Research-Atmospheres, 107, 10.1029/2000jd000176, 2002.
Wang, J., Li, M., Li, L., Zheng, R., Fan, X., Hong, Y., Xu, L., Chen, J., and Hu, B.: Particle number size distribution and new particle formation in Xiamen, the coastal city of Southeast China in wintertime, Science of the Total Environment, 826, 154208, 10.1016/j.scitotenv.2022.154208, 2022.
Wang, M. L., Chen, Y. Q., Fu, H. Y., Qu, X. L., Shen, G. F., Li, B. G., and Zhu, D. Q.: Combined analyses of hygroscopic properties of organic and inorganic components of three representative black carbon samples recovered from pyrolysis, Science of the Total Environment, 771, 10.1016/j.scitotenv.2021.145393, 2021.
Wang, Y., Li, J., Fang, F., Zhang, P., He, J., Pöhlker, M. L., Henning, S., Tang, C., Jia, H., Wang, Y., Jian, B., Shi, J., and Huang, J.: In-situ observations reveal weak hygroscopicity in the Southern Tibetan Plateau: implications for aerosol activation and indirect effects, npj Climate and Atmospheric Science, 7, 77, 10.1038/s41612-024-00629-x, 2024.
Won, W. S., Oh, R., Lee, W., Ku, S., Su, P. C., and Yoon, Y. J.: Hygroscopic properties of particulate matter and effects of their interactions with weather on visibility, Scientific Reports, 11, 10.1038/s41598-021-95834-6, 2021.
Wu, S. P., Schwab, J., Yang, B. Y., Zheng, A., and Yuan, C. S.: Two-Years PM2.5 Observations at Four Urban Sites along the Coast of Southeastern China, Aerosol and Air Quality Research, 15, 1799-1812, 10.4209/aaqr.2015.05.0363, 2015a.
Wu, S. P., Cai, M. J., Xu, C., Zhang, N., Zhou, J. B., Yan, J. P., Schwab, J. J., and Yuan, C. S.: Chemical nature of PM2.5 and PM10 in the coastal urban Xiamen, China: Insights into the impacts of shipping emissions and health risk, Atmospheric Environment, 227, 10.1016/j.atmosenv.2020.117383, 2020.
Wu, Y. F., Wang, X. J., Yan, P., Zhang, L. M., Tao, J., Liu, X. Y., Tian, P., Han, Z. W., and Zhang, R. J.: Investigation of hygroscopic growth effect on aerosol scattering coefficient at a rural site in the southern North China Plain, Science of the Total Environment, 599, 76-84, 10.1016/j.scitotenv.2017.04.194, 2017.
Wu, Z. J., Poulain, L., Birmili, W., Gröss, J., Niedermeier, N., Wang, Z. B., Herrmann, H., and Wiedensohler, A.: Some insights into the condensing vapors driving new particle growth to CCN sizes on the basis of hygroscopicity measurements,

963 Atmospheric Chemistry and Physics, 15, 13071-13083, 10.5194/acp-15-13071-2015,
964 2015b.
965 Wu, Z. J., Zheng, J., Shang, D. J., Du, Z. F., Wu, Y. S., Zeng, L. M., Wiedensohler, A.,
966 and Hu, M.: Particle hygroscopicity and its link to chemical composition in the urban
967 atmosphere of Beijing, China, during summertime, Atmospheric Chemistry and
968 Physics, 16, 1123-1138, 10.5194/acp-16-1123-2016, 2016.
969 Wu, Z. J., Wang, Y., Tan, T. Y., Zhu, Y. S., Li, M. R., Shang, D. J., Wang, H. C., Lu, K.
970 D., Guo, S., Zeng, L. M., and Zhang, Y. H.: Aerosol Liquid Water Driven by
971 Anthropogenic Inorganic Salts: Implying Its Key Role in Haze Formation over the
972 North China Plain, Environmental Science & Technology Letters, 5, 160-166,
973 10.1021/acs.estlett.8b00021, 2018.
974 Xia, C., Sun, J. Y., Qi, X. F., Shen, X. J., Zhong, J. T., Zhang, X. Y., Wang, Y. Q., Zhang,
975 Y. M., and Hu, X. Y.: Observational study of aerosol hygroscopic growth on scattering
976 coefficient in Beijing: A case study in March of 2018, Science of the Total Environment,
977 685, 239-247, 10.1016/j.scitotenv.2019.05.283, 2019.
978 Xia, C., Sun, J. Y., Hu, X. Y., Shen, X. J., Zhang, Y. M., Zhang, S. A., Wang, J. L., Liu,
979 Q., Lu, J. Y., Liu, S., and Zhang, X. Y.: Effects of hygroscopicity on aerosol optical
980 properties and direct radiative forcing in Beijing: Based on two-year observations,
981 Science of the Total Environment, 857, 10.1016/j.scitotenv.2022.159233, 2023.
982 Xu, L. L., Duan, F. K., He, K. B., Ma, Y. L., Zhu, L. D., Zheng, Y. X., Huang, T., Kimoto,
983 T., Ma, T., Li, H., Ye, S. Q., Yang, S., Sun, Z. L., and Xu, B. Y.: Characteristics of the
984 secondary water-soluble ions in a typical autumn haze in Beijing, Environmental
985 Pollution, 227, 296-305, 10.1016/j.envpol.2017.04.076, 2017a.
986 Xu, W., Guo, S., Gomez-Hernandez, M., Zamora, M. L., Secrest, J., Marrero-Ortiz, W.,
987 Zhang, A. L., Collins, D. R., and Zhang, R. Y.: Cloud forming potential of oligomers
988 relevant to secondary organic aerosols, Geophysical Research Letters, 41, 6538-6545,
989 10.1002/2014gl061040, 2014.
990 Xu, W. Q., Han, T. T., Du, W., Wang, Q. Q., Chen, C., Zhao, J., Zhang, Y. J., Li, J., Fu,
991 P. Q., Wang, Z. F., Worsnop, D. R., and Sun, Y. L.: Effects of Aqueous-Phase and
992 Photochemical Processing on Secondary Organic Aerosol Formation and Evolution in
993 Beijing, China, Environmental Science & Technology, 51, 762-770,
994 10.1021/acs.est.6b04498, 2017b.
995 Yan, P., Pan, X. L., Tang, J., Zhou, X. J., Zhang, R. J., and Zeng, L. M.: Hygroscopic
996 growth of aerosol scattering coefficient: A comparative analysis between urban and
997 suburban sites at winter in Beijing, Particuology, 7, 52-60, 10.1016/j.partic.2008.11.009,
998 2009.
999 Yu, Y. L., Zhao, C. S., Kuang, Y., Tao, J. C., Zhao, G., Shen, C. Y., and Xu, W. Y.: A
1000 parameterization for the light scattering enhancement factor with aerosol chemical
1001 compositions, Atmospheric Environment, 191, 370-377,
1002 10.1016/j.atmosenv.2018.08.016, 2018.
1003 Yue, D. L., Hu, M., Zhang, R. Y., Wang, Z. B., Zheng, J., Wu, Z. J., Wiedensohler, A.,
1004 He, L. Y., Huang, X. F., and Zhu, T.: The roles of sulfuric acid in new particle formation

and growth in the mega-city of Beijing, Atmospheric Chemistry and Physics, 10, 4953-4960, 10.5194/acp-10-4953-2010, 2010.
Zhang, L., Sun, J. Y., Shen, X. J., Zhang, Y. M., Che, H., Ma, Q. L., Zhang, Y. W., Zhang, X. Y., and Ogren, J. A.: Observations of relative humidity effects on aerosol light scattering in the Yangtze River Delta of China, Atmospheric Chemistry and Physics, 15, 8439-8454, 10.5194/acp-15-8439-2015, 2015.
Zhang, Q., Zheng, Y. X., Tong, D., Shao, M., Wang, S. X., Zhang, Y. H., Xu, X. D., Wang, J. N., He, H., Liu, W. Q., Ding, Y. H., Lei, Y., Li, J. H., Wang, Z. F., Zhang, X. Y., Wang, Y. S., Cheng, J., Liu, Y., Shi, Q. R., Yan, L., Geng, G. N., Hong, C. P., Li, M., Liu, F., Zheng, B., Cao, J. J., Ding, A. J., Gao, J., Fu, Q. Y., Huo, J. T., Liu, B. X., Liu, Z. R., Yang, F. M., He, K. B., and Hao, J. M.: Drivers of improved PM2.5 air quality in China from 2013 to 2017, Proceedings of the National Academy of Sciences of the United States of America, 116, 24463-24469, 10.1073/pnas.1907956116, 2019.
Zhao, C. S., Yu, Y. L., Kuang, Y., Tao, J. C., and Zhao, G.: Recent Progress of Aerosol Light-scattering Enhancement Factor Studies in China, Advances in Atmospheric Sciences, 36, 1015-1026, 10.1007/s00376-019-8248-1, 2019a.
Zhao, P. S., Ding, J., Du, X., and Su, J.: High time-resolution measurement of light scattering hygroscopic growth factor in Beijing: A novel method for high relative humidity conditions, Atmospheric Environment, 215, 10.1016/j.atmosenv.2019.116912, 2019b.
Zheng, B., Tong, D., Li, M., Liu, F., Hong, C. P., Geng, G. N., Li, H. Y., Li, X., Peng, L. Q., Qi, J., Yan, L., Zhang, Y. X., Zhao, H. Y., Zheng, Y. X., He, K. B., and Zhang, Q.: Trends in China's anthropogenic emissions since 2010 as the consequence of clean air actions, Atmospheric Chemistry and Physics, 18, 14095-14111, 10.5194/acp-18-14095-2018, 2018.
Zhou, S. Z., Wu, L. L., Guo, J. C., Chen, W. H., Wang, X. M., Zhao, J., Cheng, Y. F., Huang, Z. Z., Zhang, J. P., Sun, Y. L., Fu, P. Q., Jia, S. G., Tao, J., Chen, Y. N., and Kuang, J. X.: Measurement report: Vertical distribution of atmospheric particulate matter within the urban boundary layer in southern China - size-segregated chemical composition and secondary formation through cloud processing and heterogeneous reactions, Atmospheric Chemistry and Physics, 20, 6435-6453, 10.5194/acp-20-6435-2020, 2020.
Zieger, P., Fierz-Schmidhauser, R., Gysel, M., Strom, J., Henne, S., Yttri, K. E., Baltensperger, U., and Weingartner, E.: Effects of relative humidity on aerosol light scattering in the Arctic, Atmospheric Chemistry and Physics, 10, 3875-3890, 10.5194/acp-10-3875-2010, 2010.
Zieger, P., Fierz-Schmidhauser, R., Weingartner, E., and Baltensperger, U.: Effects of relative humidity on aerosol light scattering: results from different European sites, Atmospheric Chemistry and Physics, 13, 10609-10631, 10.5194/acp-13-10609-2013, 2013.
Zieger, P., Fierz-Schmidhauser, R., Poulain, L., Muller, T., Birmili, W., Spindler, G., Wiedensohler, A., Baltensperger, U., and Weingartner, E.: Influence of water uptake on

1047 the aerosol particle light scattering coefficients of the Central European aerosol, Tellus
1048 Series B-Chemical and Physical Meteorology, 66, 10.3402/tellusb.v66.22716, 2014.
1049